Geophysical Research Letters

RESEARCH LETTER
10.1029/2025GL115543

Extended Duration of Abrupt Climate Events From the Early to Late Holocene

Y. Liu[1,2], C. Hu[1], Z. Hu[1], J. Liao[3], M. Liang[4], and Q. Yin[4]

[1]Hubei Key Laboratory of Regional Ecology and Environmental Change, School of Geography and Information Engineering, China University of Geosciences, Wuhan, China, [2]Faculty of Materials Science and Chemistry, China University of Geosciences, Wuhan, China, [3]Wuhan Center of China Geological Survey, Wuhan, China, [4]Earth and Climate Research Center, Earth and Life Institute, Université Catholique de Louvain, Louvain-la-Neuve, Belgium

Key Points:

- The first continuous annually resolved stalagmite $\delta^{18}O$ record of the 4.2 ka event from East Asian Monsoon domain
- Abrupt climate events show an extended duration with a similar asymmetric double-pulse structure from the early to late Holocene
- The extended event duration is related to the decreasing boreal summer insolation and sea ice change in the North Atlantic

Supporting Information:

Supporting Information may be found in the online version of this article.

Correspondence to:

Y. Liu,
yhliu@cug.edu.cn

Citation:

Liu, Y., Hu, C., Hu, Z., Liao, J., Liang, M., & Yin, Q. (2025). Extended duration of abrupt climate events from the early to late Holocene. *Geophysical Research Letters*, *52*, e2025GL115543. https://doi.org/10.1029/2025GL115543

Received 21 FEB 2025
Accepted 27 MAR 2025

Author Contributions:

Conceptualization: Y. Liu, C. Hu, Q. Yin
Formal analysis: M. Liang
Funding acquisition: Y. Liu, C. Hu
Investigation: Y. Liu, C. Hu, J. Liao
Methodology: Y. Liu, C. Hu, Z. Hu, J. Liao, M. Liang, Q. Yin
Resources: C. Hu, M. Liang
Supervision: C. Hu
Validation: Y. Liu, C. Hu, Z. Hu, J. Liao, Q. Yin
Writing – original draft: Y. Liu
Writing – review & editing: Y. Liu

Abstract Due to the lack of continuous annual records of Holocene climate events, their evolution remains unclear. In this study, we present a new annually resolved stalagmite oxygen isotope ($\delta^{18}O$) record covering the 4.2 ka event from the East Asian monsoon domain, and compare it with two annually resolved $\delta^{18}O$ records of the 8.2 ka event and the Little Ice Age from the same stalagmite. These abrupt events share a similar asymmetric double-pulse structure, but exhibit extended event duration with less extreme climate excursion from the early to late Holocene. Climate simulations suggest that the changes in duration and frequency of the abrupt events could be related to the variations of East Asian summer monsoon and summer sea surface temperature in the North Atlantic. The waxing and waning of sea ice in the North Atlantic induced by Holocene summer insolation and atmosphere-ocean internal variability may contribute to differences in event duration.

Plain Language Summary The study of past climate events can provide important information for possible future abrupt climate change. However, only records with annual resolution can reveal the characteristics of climate events in detail. The lack of continuous annual records makes it difficult to explore climate evolution over the past 9,000 years. This study provides a record of the first annually resolved climate record of stalagmite oxygen isotope from the East Asia monsoon region around 4,200 years ago. To avoid the uncertainties introduced by different resolutions, proxies, and locations, this new record was compared with two other annually resolved event records around 8,200 and 300 years ago based on the same proxy and the same stalagmite using an objective event limiting method. An extended event duration with less extreme climate under decreasing boreal summer insolation from the early to late Holocene is presented, which is also supported by climate simulations. The change of sea ice in the North Atlantic under different insolation and atmosphere-ocean internal variability may contribute to the differing duration of events. The new findings suggest that under the influence of ongoing global warming, abrupt climate events may become shorter but more extreme and with higher frequency.

1. Introduction

During the Holocene, it appears that a series of North Atlantic cooling events called Bond events (Bond et al., 1997), played a key role in global climate change (Bond et al., 2001; Gupta et al., 2003), leading to weakening of the Asian monsoon (Gupta et al., 2003; Tan et al., 2020; Wang et al., 2016) and extreme droughts (Griffiths et al., 2020; Weiss & Bradley, 2001), strongly affecting regional ecosystems and environments (Di Rita & Magri, 2009; Griffiths et al., 2020; Lu et al., 2019). Understanding their evolution and mechanisms may provide important clues for the prediction of abrupt climate change and disaster risk reduction under global warming.

Though these generally cold and dry events have been widely recorded in different geological archives (e.g., Duan F. et al., 2023; Kobashi et al., 2017; Sicre et al., 2021), due to limitations in comparing different event records, it remains difficult to reveal the broad picture of Holocene events. A statistical analysis of six Holocene events from Bond 5 (8.2 ka event) to Bond 0 (LIA: Little Ice Age) showed no clear spatio-temporal pattern or cyclicity of the climate events, due to the uncertainties related to chronology, resolution, proxies and locations (Wanner et al., 2011). The lack of highly resolved Holocene records and the complexity of the paleoclimate data also fail to reveal significant global influence of most Bond events (Mckay et al., 2024). Even highly resolved Holocene records from interannual to decadal scales show large discrepancies during different climate events (Duan F. et al., 2023; Hu et al., 2008; Kobashi et al., 2017; Sicre et al., 2021; Wang et al., 2005) (Figure S1 in Supporting

Information S1). Studies on individual climate events, for example, the 8.2 ka event, do present a generally similar double-pulse structure from different locations (Duan F. et al., 2023; Sicre et al., 2021; Wang et al., 2005). However, due to the lack of comparable annually resolved records of other Bond events, it is still difficult to detect the amplitude, periodicity and duration of these events in most records.

Chinese stalagmite oxygen isotope ($\delta^{18}O$) appears to be sensitive to changes in global climate (Cheng et al., 2016; Duan F., 2023; Hu et al., 2008; Wang et al., 2005), especially to Asian summer monsoon variation. Without precipitation, stalagmites will not grow, thus, stalagmites can record variations in precipitation $\delta^{18}O$. Modern rainfall monitoring shows that monthly rainfall $\delta^{18}O$ in the East Asian Monsoon (EAM) region is significantly correlated to all monsoon indices (Wang et al., 2020). Studies also show that Chinese stalagmite oxygen isotopes are influenced by Asian monsoon (Wang et al., 2022; Zhao et al., 2023). During Bond events, a weakening monsoon is accompanied by attenuated upstream effects, leading to a positive precipitation $\delta^{18}O$ (Wang et al., 2020), then being recorded by stalagmite $\delta^{18}O$. It is believed that Bond events are related to the slowing of the Atlantic Meridional Overturning Circulation (AMOC) induced by ice melting and freshwater discharge into the North Atlantic (Alley & Agustsdottir, 2005; Morrill et al., 2014; Rashid et al., 2023; Yan & Liu, 2019), and the decline of AMOC related to weakening of Asian summer monsoon could be imprinted in Chinese stalagmite $\delta^{18}O$ (Zhao et al., 2023). These studies suggest that the timing of Bond events could be anchored by stalagmite $\delta^{18}O$ from the EAM domain, and address the lack of annually resolved records from the North Atlantic during the Holocene.

Previous studies have shown that the annually resolved $\delta^{18}O$ records from laminated stalagmites with precise relative chronology from the EAM domain could record the characteristics of the 8.2 ka event (Bond 5) giving precise details of duration and structure, helping to relate variations to North Atlantic climate change (Duan P. et al., 2023; Liu et al., 2013). In addition to the Bond 5 event, to better understand the event structure during the Holocene, it would be helpful to obtain detailed information of abrupt changes caused by other Bond events. An apparent existing problem is that different stalagmite $\delta^{18}O$ records with interannual to decadal resolutions show different behavior for a given Bond event (Figure S1c–S1e in Supporting Information S1). A major reason is that these records are from different caves with different resolutions. Though ensemble data analysis of stalagmite $\delta^{18}O$ from EAM regions could better isolate the monsoon signal (Wang et al., 2022), all the selected sequences must have a similar resolution. The lack of annually resolved stalagmite $\delta^{18}O$ records during each Bond event in the EAM region makes comparison exceedingly challenging. A possible approach is to obtain at least three event records with the same annual resolution and precise chronology covering the early, middle and late Holocene respectively from a common sample. The climate events that receive most attention are the 8.2 ka, 4.2 ka and the Little Ice Age (LIA) events. The 8.2 ka and the 4.2 ka events mark the boundaries of the early/middle and middle/late Holocene respectively (Walker et al., 2012), while the LIA is the cooling event closest to the present (Matthews & Briffa, 2005). In addition, the 8.2 ka event is the most prominent during the whole Holocene (Vinther et al., 2006), whilst the 4.2 ka event is suggested to be related to the collapse of Neolithic cultures around the world (Weiss et al., 1993). For the LIA, it is a key period to assess the roles of natural and anthropogenic forcing (Mann et al., 2009). Significantly, the three events are under different climate boundary conditions, which have been widely applied in climate simulations (Drijfhout et al., 2013; Morrill et al., 2014; Yan & Liu, 2019).

A stalagmite covering a series of Holocene events, named HS4, from central China (30°27' N, 110°250' E; 294 m) was selected for this study (Hu et al., 2008). Based on two published HS4 $\delta^{18}O$ records during the 8.2 ka (Liu et al., 2013) and the LIA (Wang et al., 2022), further measurements were made of HS4 $\delta^{18}O$ at annual intervals during the 4.2 ka event (Bond 3), to build a link between the early and the late Holocene. The new record during the 4.2 ka is the first continuous, annually resolved stalagmite $\delta^{18}O$ record of the 4.2 ka event in East Asia. Precise comparisons between the three high resolution records from the same stalagmite makes it possible to explore the evolution of climate events from the early to late Holocene.

2. Results

2.1. Annual Stalagmite $\delta^{18}O$ Record of HS4 During the 4.2 ka Event

Based on the published decadal $\delta^{18}O$ anomaly around the 4.2 ka in stalagmite HS4 (Hu et al., 2008), the section at measured position 147.69–125.12 cm with clear annual layering was selected to ensure the whole event was included (Figure 1). The chronology of this section was established by a combination of layer counting and U-Th dating. The layer counting was anchored by its top layer as the year of collection, 2001 AD. This 4.2 ka section

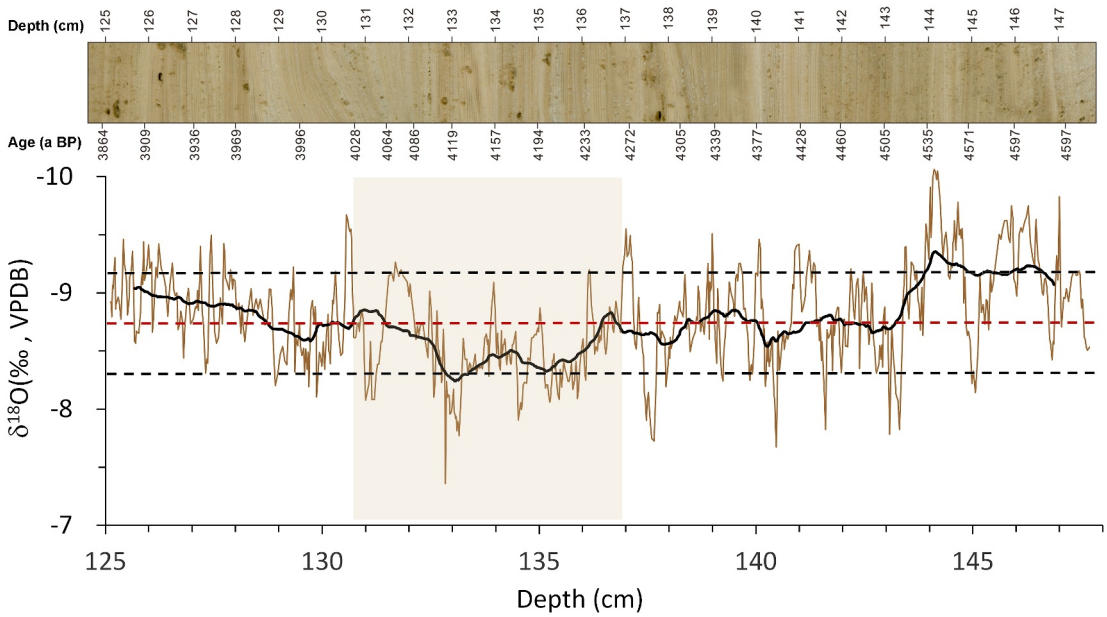

Figure 1. Annually resolved record of HS4 $\delta^{18}O$ in depth of 148–125 cm and the HS4 profile image with marked chronology sequence. The polished profile of HS4 displays a laminated structure, which is also the precondition for relative layer counting. The light brown shadow highlights the anomaly duration of the HS4 $\delta^{18}O$ during the whole section, indicating the 4.2 ka event was captured by HS4. The 50-year moving average of the annual HS4 $\delta^{18}O$ is shown by the bold black curve, which demonstrates a double-pulse structure in the light brown shadow. The ±1 SD and the average of HS4 $\delta^{18}O$ in this section are shown in black and red dashed lines respectively.

from 147.69 to 125.12 cm contains a total of 779 layers spanning the period from 4,649 to 3,871 a BP as shown in Figure S2 in Supporting Information S1. Though the absolute chronological uncertainty is approximately 60 years measured by U-Th dating (Hu et al., 2008) and approximately 30 years from the accumulated errors of the layer counting from the top layer to the 4.2 ka section, the relative chronology within the selected section is more precise with a layer counting error of less than 10 years, ensuring the complete 4.2 ka event is well characterized, and the event structure is accurate enough to allow comparison with other events. After sampling for $\delta^{18}O$ measurement (Text S4 in Supporting Information S1), an annual $\delta^{18}O$ sequence of HS4 from 4.65 to 3.87 ka BP was established (Figure 1). The values of $\delta^{18}O$ in this section range from −10.07‰ to −7.36‰ with an average of −8.76‰ and a standard deviation (SD) of 0.42‰. The 50-year moving average presents a higher $\delta^{18}O$ duration between 4.27 ka BP (136.94 cm) and 4.05 ka BP (130.66 cm) (Figure 1), demonstrating that the 4.2 ka event was effectively captured by HS4. After 4.27 ka BP, the HS4 $\delta^{18}O$ increases until more than 1 SD above the average, followed by intense fluctuations with two prominent anomalies around 4.21 ka BP (135.34 cm) and 4.12 ka BP (133.02 cm) (Figure 1), and then returned to 1 SD below the average. Generally, the 4.2 ka event in HS4 presents a double-pulse pattern (light brown shadow in Figure 1).

2.2. Comparison Between the 4.2 ka, 8.2 ka, and LIA Events

Since different event definition methods result in different event durations, to approach an objective criterion for identifying the 4.2 ka, 8.2 ka and LIA events to allow comparability among the three events, it is necessary to set a reference period for each event, then view an event in terms of its deviation away from the calculated average for the reference period. A useful strategy is to identify the duration of the dominant cycle of each event, and to set an equal number of cycles to be the reference period for each event. Spectral analysis of HS4 $\delta^{18}O$ reveals the dominant cycles of the 8.2 ka, 4.2 ka and the LIA events of ∼60, 90 and 110 years respectively (Figure S3 in Supporting Information S1). Considering the length of each record, we determined to set the reference period to be 5 climate cycles for each event (details are shown in Figures S3 and S4 and Texts S5 and S6 in Supporting Information S1). In the following text, the average and 1SD values of $\delta^{18}O$ are calculated based on a reference period of 5 dominant cycles of each event. In this way, the full span of the event is included for the 8.2 ka, 4.2 ka and LIA. The gray shaded areas in Figure 2 indicate the total duration of the three events, with the 30-year moving average $\delta^{18}O$ reaching its lowest before and after crossing the average $\delta^{18}O$ of each reference period, indicating

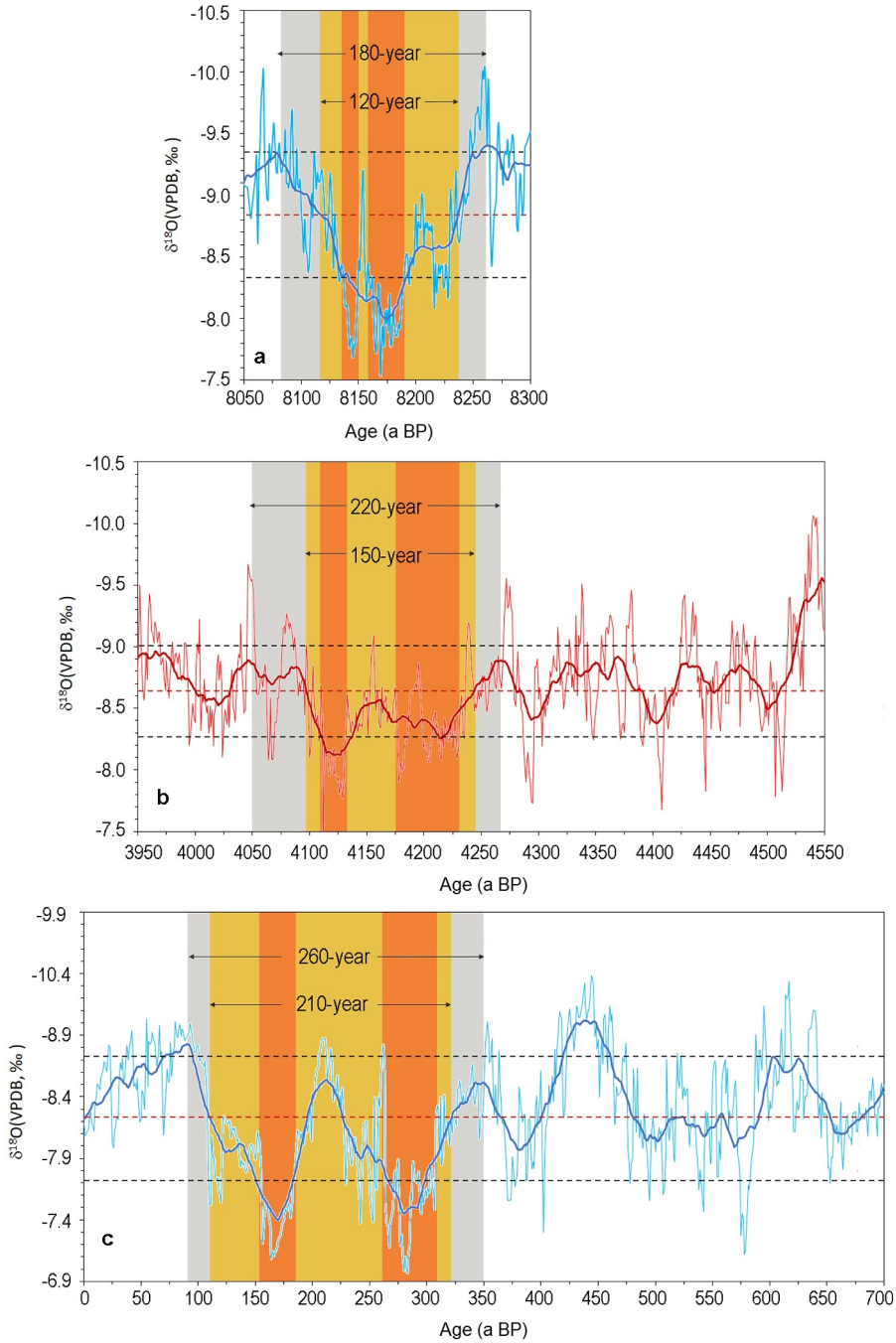

Figure 2. Comparison between the 8.2 ka, 4.2 ka and the LIA events based on the HS4 $\delta^{18}O$ records. (a–c) Annual HS4 $\delta^{18}O$ records (thin curve) with the 30-year moving average (bolder curve) during the 8.2 ka (Liu et al., 2013), 4.2 ka (this study) and the LIA (Wang et al., 2022). The full and central duration of each event are indicated by a gray and a yellow shading. The horizontal red and the black dashed lines in each figure mark the calculated average and ±1 SD of the $\delta^{18}O$ values based on a reference period of 5 climate cycles of each event, which are 310, 470 and 540 years for the 8.2 ka,4.2 ka and LIA event respectively (details are shown in Figure S4 in Supporting Information S1). The two anomalies where the 30-year moving average $\delta^{18}O$ values are more positive than the 1 SD level are marked by orange shadows.

the duration of LIA (~260 years) as the longest, compared with the 4.2 ka (~220 years) and 8.2 ka events (~180 years), and suggest a lengthening trend of event duration from the early to late Holocene. The yellow shaded areas in Figure 2 mark the central periods of the three events, with the 30-year moving average $\delta^{18}O$ higher than the average $\delta^{18}O$ of each reference period, demonstrating a longer central duration of the LIA (~210 years),

compared to the 4.2 ka (~150 years) and the 8.2 ka event (~120 years). It also indicates that the central period of each event covers nearly 2 dominant cycles, though the central duration of the 4.2 ka event is a bit shorter. Thus, it might be conjectured that the dominant cycle controls each event duration.

Generally, the $\delta^{18}O$ values during each event display an increase at the beginning, followed by two prominent anomalies, ending with a decreasing trend until the $\delta^{18}O$ values recover to the equivalent level preceding the event (Figure 2). In each case, the two anomalies can be identified where the 30-year moving average $\delta^{18}O$ passes the 1 SD level, and the first anomaly lasts longer than the later, second one (orange shadows in Figure 2). Between the two anomalies, there is a rebound, which could be observed in each annual record. During the 8.2 ka event, the $\delta^{18}O$ rebound is the sharpest among the three events, it does not touch the 1SD line below the average, and its duration is the shortest. The rebound signals in both the 4.2 ka and LIA events cross the 1SD line below the average, and account for ~30% and 40% of their central event duration respectively (~10% during the 8.2 ka), suggesting the relative rebound duration in the LIA is the longest. Following the 30-year moving average, the rebound signals in the 4.2 ka and LIA remain visible, whilst the amplitude of the rebound is the largest in the LIA among the three events (Figure 2c). As a proportion of the whole event, the duration of the central extreme in each event becomes smaller from early to late Holocene. In summary, the three events present a similar asymmetric double-pulse structure marked by two prominent anomalies with an extending duration and a reducing extreme condition from the early to late Holocene.

3. Discussion

3.1. Event Cycles Revealed by Climate Simulations

To explore the possible causes of the varying event cycles during the 8.2 ka, 4.2 ka and LIA events, we analyzed the model outputs of the TraCE21 ka (Simulation of Transient Climate Evolution over the last 21,000 years) (Liu et al., 2014). The duration selected for the spectrum analysis on the simulated data during each event are the same as on HS4 $\delta^{18}O$, which are from 8.29 to 8.06, 4.30–3.95, and 0.50–0 ka BP, with a similar confidence level of 90%. As observed in HS4 $\delta^{18}O$ records, under the effect of orbital forcing, both the simulated intensity of the East Asian summer monsoon (EASM) (Figures 3d–3f) and the North Atlantic (NA) summer sea surface temperature (SST) display extending cycles from the 8.2 ka to the LIA event (Figures 3g–3i). Moreover, the consistent cycles of ~60, 90 and over 100 years in the simulated EASM and North Atlantic summer SST as well as in the HS4 $\delta^{18}O$ records during the 8.2 ka, 4.2 ka and LIA events (Figure 3) suggest a common driving force and/or a strong teleconnection between the North Atlantic climate and the East Asian monsoon. While the decline of boreal summer insolation from the early to late Holocene could operate as a common factor, the decline of summer insolation may result in a long-term cooling and cycle change in the North Atlantic which could in turn affect the EASM. Previous studies have shown that a cooling in the North Atlantic could produce an eastward propagating wave train across the mid-latitudes of Eurasia (Wu et al., 2022), reinforcing the cooling across the Northern Hemisphere, and cause a southward shift of the Intertropical Convergence Zone (ITCZ), resulting in a weakening of the EASM (Ning et al., 2019) and an increase of rainfall $\delta^{18}O$ in the EAM domain (Wang et al., 2020), finally being recorded by stalagmite $\delta^{18}O$ (Wang et al., 2005).

3.2. Synchronous Variations Between the North Atlantic Summer SST and HS4 $\delta^{18}O$

Proxy-based paleoclimate reconstructions from the North Atlantic also suggest a teleconnection with the HS4 $\delta^{18}O$. Figure 4 shows that following the boreal summer insolation decline (Berger & Loutre, 1991), the reconstructed sea ice around the Fram Strait, the major gateway connecting the Arctic and the North Atlantic, demonstrates a gradually increasing trend from the early to the late Holocene (Figure 4a), and the summer SST record from the western Nordic Seas with an average resolution of ~4 years presents a decreasing trend (Figure 4b). Both the sea ice expansion and the summer SST decrease in the North Atlantic are synchronous with a general increasing trend of the decadal HS4 $\delta^{18}O$ in the past 9,000 years (Figure 4c). Moreover, the HS4 annual $\delta^{18}O$ variations during the 8.2 ka (Liu et al., 2013), 4.2 ka and LIA (Wang et al., 2022) events also generally match with the high-resolution summer SST record in the North Atlantic (Sicre et al., 2021) within their chronological uncertainties. There appears to be an anti-phase relationship between them during each event (Figure 4d), supporting a link between boreal summer insolation, the North Atlantic summer SST and the EASM as deduced during each event from the TraCE-Orb simulation (Figure 3). The comparable variations between the HS4 $\delta^{18}O$ in

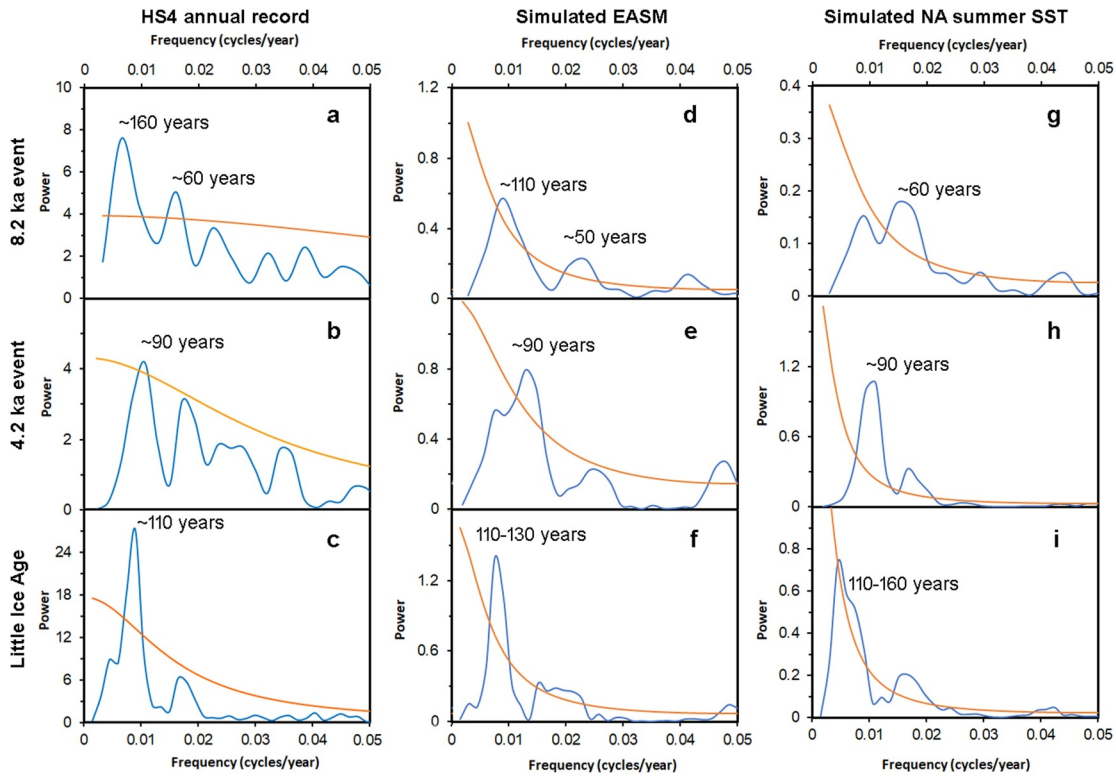

Figure 3. Periodicity analysis by REDFIT (Schulz & Mudelsee, 2002) on HS4 $\delta^{18}O$ record with the North Atlantic summer SST and EASM simulated by TraCE-Orb. (a–c) Cycles of annual HS4 $\delta^{18}O$ records during the 8.2 ka, 4.2 ka and LIA events. (d–f) Cycles of simulated EASM by TraCE-Orb during the 8.2 ka, 4.2 ka and LIA events. (g–i) Cycles of simulated North Atlantic (NA) summer SST by TraCE-Orb during the 8.2 ka, 4.2 ka and LIA events. The blue and yellow lines show the power variation and 90% confidence levels of each data set respectively. All the HS4 $\delta^{18}O$, simulated EASM and North Atlantic summer SST reveal similar cycles during each event.

the EAM region and the summer SST around the North Atlantic during the three events also indicate that HS4 $\delta^{18}O$ has the potential to anchor the North Atlantic events at high resolution.

Besides the atmospheric transport processes mentioned above, the response of stalagmite $\delta^{18}O$ in East Asia to the North Atlantic cooling could possibly be bridged by AMOC, a crucial component of oceanic circulation (McCarthy et al., 2012), as the occurrence of Bond events appear related to the slowdown of AMOC, including the 8.2 ka (Alley & Agustsdottir, 2005; Cheng et al., 2009; Clarke et al., 2004; Morrill et al., 2014), 4.2 ka (Lin et al., 2022; Yan & Liu, 2019) and LIA (Rashid et al., 2023) events, which can impact the North Atlantic climate by weakening the poleward heat transport (Sévellec et al., 2017), leading to a southward shift of the ITCZ and an increase in anticyclone activity over the East Asian continent, finally causing an increase in stalagmite $\delta^{18}O$ in this region by weakening the summer monsoon (Zhao et al., 2023). The AMOC can be affected by the magnitude of freshwater input, and larger meltwater pulses may lead to a more significant slowdown of AMOC (Otto-Bliesner & Brady et al., 2010). During the 8.2 ka, there is still ice sheet cover (Clarke et al., 2004), and both the boreal summer insolation (Berger & Loutre, 1991) and summer SST (Sicre et al., 2021) are much higher than the middle and late Holocene (Figure 4b). The less dense fresh water could suppress ocean convection and interaction with the atmosphere, resulting in a cooling tongue of the atmosphere and ocean extending southwestward, leading to the formation of more sea ice by strong ice albedo feedback (Drijfhout et al., 2013). However, compared with the 8.2 ka, from the 4.2 ka to LIA, there are no remnant ice sheets (Lambeck et al., 2014), and the insolation (Berger & Loutre, 1991) and summer SST (Sicre et al., 2021) become lower (Figure 4b). Thus, the freshwater discharge anomalies during the 4.2 ka and LIA would be less prominent, which may explain the more abrupt onset of the 8.2 ka event than the other two events.

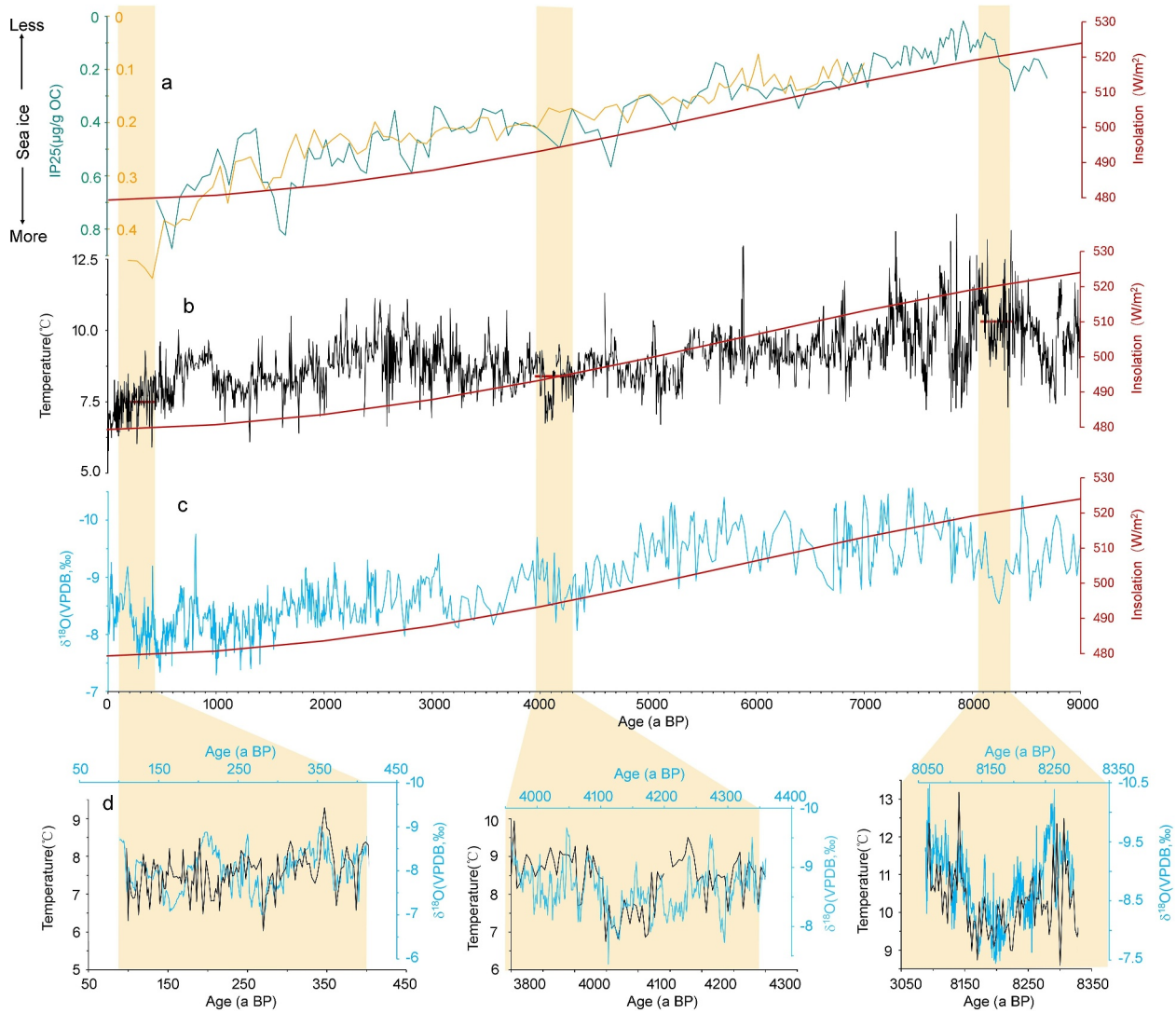

Figure 4. Comparisons of the sea ice and summer SST in North Atlantic and HS4 $\delta^{18}O$. (a–c) Comparisons between insolation at 65°N in July (Berger & Loutre, 1991) and sea ice variation (Müller et al., 2012) (a), summer SST in North Atlantic (Sicre et al., 2021) (b), and decadal HS4 $\delta^{18}O$ in the past 9,000 years (Hu et al., 2008) (c). (d) Comparisons between annual HS4 $\delta^{18}O$ records during the 8.2 ka (Liu et al., 2013), 4.2 ka (this study) and LIA (Wang et al., 2022) (blue) with North Atlantic summer SST (Sicre et al., 2021) (black). The sea ice reconstructions based on proxy IP25 in green and yellow are from sediment cores MSM5/5-712-2 and MSM5/5-723-2 (Müller et al., 2012). The yellow shadows highlight the variations during the 8.2 ka, 4.2 ka and LIA events. The horizonal short red lines are the averages of SST during the 8.2 ka (10.1°C), 4.2 ka (8.1°C) and LIA (7.5°C) events respectively.

3.3. Influence of North Atlantic Sea Ice on the Event Duration

Different climate backgrounds could also affect the recovery time following a climate event. Figure 4a shows that the sea ice in the North Atlantic expanded from early to late Holocene, and reached a maximum at the LIA (Müller et al., 2012), which is supported by other studies in this region (Justwan & Koç, 2008; Vare et al., 2009). The boreal summer insolation declines from 8.2 ka to the LIA (Berger & Loutre, 1991) leading to decreasing summer SST (Sicre et al., 2021) and increasing sea ice which could then act to slow down the rate of sea ice melting and so lengthen the event recovery time. In this scenario, during the 8.2 ka event, with high summer insolation (Berger & Loutre, 1991), high summer SST (Sicre et al., 2021) and less sea ice (Müller et al., 2012) in the North Atlantic, the sea ice melting rate would be much faster than for the 4.2 ka and the LIA events. In addition, during the early Holocene, high seasonality induced warmer summers (Screen & Francis, 2016), strong hydrofracture propagation in ice sheets (Chandler & Hubbard, 2023), and more bursting of pressurized bubbles from sea ice (Wengrove et al., 2023) under higher summer insolation, which would further accelerate the rate of sea ice melting. The loss

of the sea ice accompanied by weak albedo feedback and intense evaporation, could result in an increase of upper ocean salinity in the North Atlantic, which might further contribute to a fast AMOC recovery (Huang et al., 2015; Nobre et al., 2023) during the 8.2 ka.

In contrast, during the LIA, under a lower boreal summer insolation (Berger & Loutre, 1991), low SST (Sicre et al., 2021), and more sea ice cover (Müller et al., 2012) around the North Atlantic, melting of sea ice would need more energy. However, both heat and energy deposited in the upper ocean are lower compared to the 8.2 ka and the 4.2 ka, resulting in a lower rate of sea ice melting and longer event recovery duration in LIA. The slower rate of sea ice melting and weaker evaporation would operate to prevent the upper ocean salinity increasing in North Atlantic, then lengthening the AMOC recovery time (Huang et al., 2015) and the duration of LIA. Unlike the climate background of 8.2 ka and LIA events, during the 4.2 ka, both the summer insolation and the sea ice in the North Atlantic are at medium levels (Figure 4), thus, the recovery time of the 4.2 ka is longer than the 8.2 ka, but shorter than the LIA.

Noting the northward shift of ITCZ allowed by reduced sea ice cover (Chemke et al., 2019) and a shorter AMOC recovery time, these effects may lead to a faster recovery of the EASM, with this shorter recovery being recorded by stalagmite $\delta^{18}O$ in the EAM region by a decreasing anomaly (Zhang et al., 2016). This faster event recovery during the 8.2 ka event, would appear to be opposite to the situation during the LIA, while overall we observe a trend of extended event recovery time from the 8.2 ka to the LIA. The event recovery duration change being related to the heat balance and sea ice melting rates in the North Atlantic. This is also consistent with the stretching of cycles of EASM from the 8.2 ka to the LIA simulated by TraCE21 in this study (Figure 3).

Considering the double-pulse structure in the middle of each event, the pattern lasting for ~2 cycles suggests that this double-pulse structure may be related to the North Atlantic SST according to the above simulation. A previous study successfully simulated a double-pulse structure by a TraCE-ALL view of the 4.2 ka event, proposing that the two-pulse pattern may result from internal variability, as the results derived from the TraCE-ALL experiment differ from any single forcing sensitivity experiment (Yan & Liu, 2019). Further climate simulations suggest that an abrupt cooling, for example, with an anomaly similar to that of the Little Ice Age, could arise spontaneously by extreme anomalies in sea-ice east of Greenland, intensification of East Greenland Current, a persistent Greenland Blocking, and enhancement of the cold anomaly through regional sea-ice feedback effects (Drijfhout et al., 2013). In such an arrangement, regardless of the initial trigger, the double-pulse structure may be an inherent feature of each event, a result of two internal spontaneous atmospheric blocking–sea-ice–ocean feedback mechanisms.

4. Conclusions

An objective analysis of selected climate events based on the average and standard deviation from certain climate cycles is developed to achieve more reliable event comparisons. A new annual stalagmite $\delta^{18}O$ record from the EAM domain presents a whole and central duration of ~220 and ~150 years for the 4.2 ka event, which is longer than those of the 8.2 ka event by 40 and 30 years, and shorter than those of the LIA by 40 and 60 years based on detailed comparison using the same proxy from the same stalagmite. All three events present a similar asymmetric double-pulse structure, with the event duration increasing in length and less extreme climate excursion from the early to late Holocene. Spectrum analysis reveals three dominant cycles of ~60, 90 and 110 years during the 8.2 ka, 4.2 ka and LIA events respectively, indicating each central event experienced ~2 cycles. Consistently dominant cycles from the simulated North Atlantic summer SST and the intensity of the EASM during each event suggest that the changes in duration and frequency of the 8.2 ka, 4.2 ka and LIA events could be related to climate variations in the North Atlantic and the EAM regions. The waxing and waning of sea ice in the North Atlantic caused by Holocene summer insolation and atmosphere-ocean internal variability may contribute to different event durations. The new observation of the increasing event duration coincident with less extreme climate condition from the early to late Holocene suggest that, with ongoing global warming and accelerating ice-loss, the duration of abrupt climate events in the future may become more frequent, of shorter duration and more extreme.

Data Availability Statement

The sub-annual and annual stalagmite $\delta^{18}O$ data of HS4 were obtained from Liu et al. (2013) and Wang et al. (2022). The data of insolation at 65°N in July, North Atlantic Sea ice and summer SST, and the HS4 $\delta^{18}O$ in

the past 9,000 years were obtained from Berger and Loutre (1991), Müller et al. (2012), Sicre et al. (2021), and Hu et al. (2008) respectively. The outputs of TraCE-Orb related to the variations of East Asian summer monsoon (EASM) intensity and summer sea surface temperature (SST) in North Atlantic during the Holocene in this article can be found at https://www.earthsystemgrid.org/project/trace.html.

Acknowledgments
This work was funded by National Natural Science Foundation of China (Grants 41772368 and 41731177). We thank the reviewers for their valuable comments.

References

Alley, R. B., & Agustsdottir, A. M. (2005). The 8k event: Cause and consequences of a major Holocene abrupt climate change. *Quaternary Science Reviews*, *24*(10–11), 1123–1149. https://doi.org/10.1016/j.quascirev.2004.12.004

Berger, A., & Loutre, M. F. (1991). Insolation values for the climate of the last 10 million years. *Quaternary Science Reviews*, *10*(4), 297–317. https://doi.org/10.1016/0277-3791(91)90033-Q

Bond, G., Kromer, B., Beer, J., Muscheler, R., Evans, M. N., Showers, W., et al. (2001). Persistent solar influence on North Atlantic climate during the Holocene. *Science*, *294*(5549), 2130–2136. https://doi.org/10.1126/science.1065680

Bond, G., Showers, W., Cheseby, M., Lotti, R., Almasi, P., DeMenocal, P., et al. (1997). A pervasive millennial-scale cycle in North Atlantic Holocene and glacial climates. *Science*, *278*(5341), 1257–1266. https://doi.org/10.1126/science.278.5341.1257

Chandler, D. M., & Hubbard, A. (2023). Widespread partial-depth hydrofractures in ice sheets driven by supraglacial streams. *Nature Geoscience*, *16*(7), 605–611. https://doi.org/10.1038/s41561-023-01208-0

Chemke, R., Polvani, L. M., & Deser, C. (2019). The effect of arctic Sea Ice loss on the hadley circulation. *Geophysical Research Letters*, *46*(2), 963–972. https://doi.org/10.1029/2018GL081110

Cheng, H., Edwards, R. L., Sinha, A., Spötl, C., Yi, L., Chen, S., et al. (2016). The Asian monsoon over the past 640,000 years and ice age terminations. *Nature*, *534*(7609), 640–646. https://doi.org/10.1038/nature18591

Cheng, H., Fleitmann, D., Edwards, R. L., Wang, X., Cruz, F. W., Auler, A. S., et al. (2009). Timing and structure of the 8.2 kyr B.P. event inferred from δ^{18} O records of stalagmites from China, Oman, and Brazil. *Geology*, *37*(11), 1007–1010. https://doi.org/10.1130/G30126A.1

Clarke, G. K. C., Leverington, D. W., Teller, J. T., & Dyke, A. S. (2004). Paleohydraulics of the last outburst flood from glacial Lake Agassiz and the 8200 BP cold event. *Quaternary Science Reviews*, *23*(3–4), 389–407. https://doi.org/10.1016/j.quascirev.2003.06.004

Di Rita, F., & Magri, D. (2009). Holocene drought, deforestation and evergreen vegetation development in the central Mediterranean: A 5,500-year record from Lago Alimini Piccolo, Apulia, southeast Italy. *The Holocene*, *19*(2), 295–306. https://doi.org/10.1177/0959683608100574

Drijfhout, S., Gleeson, E., Dijkstra, H. A., & Livina, V. (2013). Spontaneous abrupt climate change due to an atmospheric blocking–sea-ice–ocean feedback in an unforced climate model simulation. *Proceedings of the National Academy of Sciences*, *110*(49), 19713–19718. https://doi.org/10.1073/pnas.1304912110

Duan, F., Zhang, Z., Liu, D., Chen, J., Shao, Q., & Wang, Y. (2023). Stalagmite-based long-term and multi-centennial hydroclimatic variations in southwestern China during the Holocene and relations to global climate change. *Quaternary Science Reviews*, *319*(21–22), 108327. https://doi.org/10.1016/j.quascirev.2023.108327

Duan, P., Li, H., Ma, Z., Zhao, J., Dong, X., Sinha, A., et al. (2023). Interdecadal to centennial climate variability surrounding the 8.2 ka event in North China revealed through an annually resolved speleothem record from Beijing. *Geophysical Research Letters*, *50*(1), 2022GL101182. https://doi.org/10.1029/2022GL101182

Griffiths, M. L., Johnson, K. R., Pausata, F. S. R., White, J. C., Henderson, G. M., Wood, C. T., et al. (2020). End of green Sahara amplified mid-to late Holocene megadroughts in mainland southeast Asia. *Nature Communications*, *11*(1), 4204. https://doi.org/10.1038/s41467-020-17927-6

Gupta, A., Anderson, D., & Overpeck, J. (2003). Abrupt changes in the Asian southwest monsoon during the Holocene and their links to the North Atlantic ocean. *Nature*, *421*(6921), 354–357. https://doi.org/10.1038/nature01340

Hu, C., Henderson, G. M., Huang, J., Xie, S., Sun, Y., & Johnson, K. R. (2008). Quantification of Holocene Asian monsoon rainfall from spatially separated cave records. *Earth and Planetary Science Letters*, *266*(3–4), 221–232. https://doi.org/10.1016/j.epsl.2007.10.015

Huang, B., Zhu, J., Marx, L., Wu, X., Kumar, A., Hu, Z., et al. (2015). Climate drift of AMOC, North Atlantic salinity and arctic sea ice in CFSv2 decadal predictions. *Climate Dynamics*, *44*(1–2), 559–583. https://doi.org/10.1007/s00382-014-2395-y

Justwan, A., & Koç, N. (2008). A diatom based transfer function for reconstructing sea ice concentrations in the North Atlantic. *Marine Micropaleontology*, *66*(3–4), 264–278. https://doi.org/10.1016/j.marmicro.2007.11.001

Kobashi, T., Menviel, L., Jeltsch-Thömmes, A., Vinther, B. M., Box, J., Muscheler, R., et al. (2017). Volcanic influence on centennial to millennial Holocene Greenland temperature change. *Science Report*, *7*, 1441. https://doi.org/10.1038/s41598-017-01451-7

Lambeck, K., Rouby, H., Purcell, A., & Sun, Y. (2014). Sea level and global ice volumes from the last glacial maximum to the Holocene. *Proceedings of the National Academy of Sciences*, *111*(43), 15296–15303. https://doi.org/10.1073/pnas.141176211

Lin, J., Jiang, W., Wang, L., Zhang, E., Tang, L., Yang, X., et al. (2022). Spatially diverse hydroclimatic response to the 4.2 ka event in the Asian monsoon region. *Quaternary Science Reviews*, *296*, 107809. https://doi.org/10.1016/j.quascirev.2022.107809

Liu, Y., Henderson, G. M., Hu, C., Mason, A. J., Charnley, N., Johnson, K. R., & Xie, S. C. (2013). Links between the East Asian monsoon and North Atlantic climate during the 8,200 year event. *Nature Geoscience*, *6*(2), 117–120. https://doi.org/10.1038/ngeo1708

Liu, Z., Zhu, J., Rosenthal, Y., Zhang, X., Otto-Bliesner, B. L., Timmermann, A., et al. (2014). The Holocene temperature conundrum. *Proceedings of the National Academy of Sciences*, *111*(34), E3501–E3505. https://doi.org/10.1073/pnas.1407229111

Lu, F., Ma, C., Zhu, C., Lu, H., Zhang, X., Huang, K., et al. (2019). Variability of East Asian summer monsoon precipitation during the Holocene and possible forcing mechanisms. *Climate Dynamics*, *52*(1–2), 969–989. https://doi.org/10.1007/s00382-018-4175-6

Mann, M. E., Zhang, Z., Rutherford, S., Bradley, R. S., Hughes, M. K., Shindell, D., et al. (2009). Global signatures and dynamical origins of the little ice age and medieval climate anomaly. *Science*, *326*(5957), 1256–1260. https://doi.org/10.1126/science.11773

Matthews, J. A., & Briffa, K. R. (2005). The 'little ice age': Re-evaluation of an evolving concept. *Geografiska Annaler - Series A: Physical Geography*, *87*(1), 17–36. https://doi.org/10.1111/j.0435-3676.2005.00242.x

McCarthy, G., Frajka-Williams, E., Johns, W. E., Baringer, M. O., Meinen, C. S., Bryden, H. L., et al. (2012). Observed inter-annual variability of the Atlantic meridional overturning circulation at 26.5ºN. *Geophysical Research Letters*, *39*(19), L19609. https://doi.org/10.1029/2012GL052933

McKay, N. P., Kaufman, D. S., Arcusa, S. H., Kolus, H. R., Edge, D. C., Erb, M. P., et al. (2024). The 4.2 ka event is not remarkable in the context of Holocene climate variability. *Nature Communications*, *15*(1), 6555. https://doi.org/10.1038/s41467-024-50886-w

Morrill, C., Ward, E. M., Wagner, A. J., Otto-Bliesner, B. L., & Rosenbloom, N. (2014). Large sensitivity to freshwater forcing location in 8.2 ka simulations. *Paleoceanography*, *29*(10), 930–945. https://doi.org/10.1002/2014PA002669

Müller, J., Werner, K., Stein, R., Fahl, K., Moros, M., & Jansen, E. (2012). Holocene cooling culminates in sea ice oscillations in Fram Strait. *Quaternary Science Reviews*, *47*(11–12), 1–14. https://doi.org/10.1016/j.quascirev.2012.04.024

Ning, L., Liu, J., Bradley, R. S., & Yan, M. (2019). Comparing the spatial patterns of climate change in the 9th and 5th millennia BP from TRACE-21 model simulations. *Climate of the Past*, *15*(1), 41–52. https://doi.org/10.5194/cp-15-41-2019

Nobre, P., Veiga, S. F., Giarolla, E., Marquez, A. L., da Silva, M. B., Capistrano, V. B., et al. (2023). AMOC decline and recovery in a warmer climate. *Scientific Reports*, *13*(1), 15928. https://doi.org/10.1038/s41598-023-43143-5

Otto-Bliesner, B. L., & Brady, E. C. (2010). The sensitivity of the climate response to the magnitude and location of freshwater forcing: Last glacial maximum experiments. *Quaternary Science Reviews*, *29*(1–2), 56–73. https://doi.org/10.1016/j.quascirev.2009.07.004

Rashid, H., Zhang, Z., Piper, D. J. W., Patro, R., & Xu, Y. (2023). Impact of medieval climate anomaly and little ice age on the labrador current flow speed and the AMOC reconstructed by the sediment dynamics and biomarker proxies. *Palaeogeography, Palaeoclimatology, Palaeoecology*, *620*, 111558. https://doi.org/10.1016/j.palaeo.2023.111558

Schulz, M., & Mudelsee, M. R. (2002). Estimatingred-noise spectra directly from unevenly spaced paleoclimatic time series. *Computers and Geosciences*, *28*(3), 421–426. https://doi.org/10.1016/S0098-3004(01)00044-9

Screen, J., & Francis, J. (2016). Contribution of sea-ice loss to Arctic amplification is regulated by Pacific Ocean decadal variability. *Nature Climate Change*, *6*(9), 856–860. https://doi.org/10.1038/nclimate3011

Sévellec, F., Fedorov, A., & Liu, W. (2017). Arctic sea-Ice decline weakens the Atlantic meridional overturning circulation. *Nature Climate Change*, *7*(8), 604–610. https://doi.org/10.1038/nclimate3353

Sicre, M. A., Jalali, B., Eiríksson, J., Knudsen, K. L., Klein, V., & Pellichero, V. (2021). Trends and centennial-scale variability of surface water temperatures in the North Atlantic during the Holocene. *Quaternary Science Reviews*, *65*(15–16), 107033. https://doi.org/10.1016/j.quascirev.2021.107033

Tan, L., Li, Y., Wang, X., Cai, Y., Lin, F., Cheng, H., et al. (2020). Holocene monsoon change and abrupt events on the western Chinese loess plateau as revealed by accurately dated stalagmites. *Geophyscial Research Letters*, *47*(21), e2020GL090273. https://doi.org/10.1029/2020GL090273

Vare, L. L., Massé, G., Gregory, T. R., Smart, C. W., & Belt, S. T. (2009). Sea ice variations in the central Canadian arctic Archipelago during the Holocene. *Quaternary Science Reviews*, *28*(13–14), 1354–1366. https://doi.org/10.1016/j.quascirev.2009.01.013

Vinther, B. M., Clausen, H. B., Johnsen, S. J., Rasmussen, S. O., Andersen, K. K., Buchar, S. L., et al. (2006). A synchronized dating of three Greenland ice cores throughout the Holocene. *Journal of Geophysical Research*, *111*(D13), D13102. https://doi.org/10.1029/2005JD006921

Walker, M. J. C., Berkelhammer, M., Björck, S., Cwynar, L. C., Fisher, D. A., Long, A. J., et al. (2012). Formal subdivision of the Holocene series/Epoch: A discussion paper by a working group of INTIMATE (integration of ice-core, marine and terrestrial records) and the subcommission on quaternary stratigraphy (international commission on stratigraphy). *Journal of Quaternary Science*, *27*(7), 649–659. https://doi.org/10.1002/jqs.2565

Wang, M., Hu, C., Liu, Y., Li, L., Xie, S., & Johnson, K. (2022). Precipitation in eastern China over the past millennium varied with large-scale climate patterns. *Communications Earth & Environment*, *3*(1), 321. https://doi.org/10.1038/s43247-022-00664-7

Wang, X., Chu, G., Sheng, M., Zhang, S., Li, J., Chen, Y., et al. (2016). Millennial-scale Asian summer monsoon variations in South China since the last deglaciation. *Earth and Planetary Science Letters*, *451*(19–20), 22–30. https://doi.org/10.1016/j.epsl.2016.07.006

Wang, Y., Cheng, H., Edwards, R. L., He, Y., Kong, X., An, Z., et al. (2005). The Holocene Asian monsoon: links to solar changes and North Atlantic climate. *Science*, *308*(5723), 854–857. https://doi.org/10.1126/science.110629

Wang, Y., Hu, C., Ruan, J., & Johnson, K. R. (2020). East Asian precipitation $\delta^{18}O$ relationship with various monsoon indices. *Journal of Geophysical Research: Atmospheres*, *125*(13), e2019JD032282. https://doi.org/10.1029/2019JD032282

Wanner, H., Solomina, O., Grosjean, M., Ritz, S. P., & Jetel, M. (2011). Structure and origin of Holocene cold events. *Quaternary Science Reviews*, *30*(21–22), 3109–3123. https://doi.org/10.1016/j.quascirev.2011.07.010

Weiss, H., & Bradley, R. S. (2001). What drives societal collapse? *Science*, *291*(5504), 609–610. https://doi.org/10.1126/science.1058775

Weiss, H., Courty, M. A., Wetterstrom, W., Guichard, F., Senior, L., Meadow, R., & Curnow, A. (1993). The genesis and collapse of third millennium north Mesopotamian civilization. *Science*, *261*(5124), 995–1004. https://doi.org/10.1126/science.261.5124.995

Wengrove, M. E., Pettit, E. C., Nash, J. D., Jackson, R. H., & Skyllingstad, E. D. (2023). Melting of glacier ice enhanced by bursting air bubbles. *Nature Geoscience*, *16*(10), 871–876. https://doi.org/10.1038/s41561-023-01262-8

Wu, J., Shi, Z., & Yang, Y. (2022). Response of East Asian summer monsoon climate to North Atlantic meltwater during the Younger Dryas. *Quaternary Science Reviews*, *295*(21–22), 107766. https://doi.org/10.1016/j.quascirev.2022.107766

Yan, M., & Liu, J. (2019). Physical processes of cooling and mega-drought during the 4.2 ka BP event: Results from TraCE-21ka simulations. *Climate of the Past*, *15*(1), 265–277. https://doi.org/10.5194/cp-15-265-2019

Zhang, H., Griffiths, M. L., Huang, J., Cai, Y., Wang, C., Zhang, F., et al. (2016). Antarctic link with East Asian summer monsoon variability during the Heinrich Stadial–Bølling interstadial transition. *Earth and Planetary Science Letters*, *453*(21–22), 243–251. https://doi.org/10.1016/j.epsl.2016.08.008

Zhao, J., Cheng, H., Cao, J., Sinha, A., Dong, X., Pan, L., et al. (2023). Orchestrated decline of Asian summer monsoon and Atlantic meridional overturning circulation in global warming period. *The Innovation Geoscience*, *1*(1), 100011–100019. https://doi.org/10.59717/j.xinn-geo.2023.100011

References From the Supporting Information

Jiang, N., Yan, Q., Xu, Z., Shi, J., & Zhang, R. (2020). The meridional shift of the midlatitude westerlies over arid central Asia during the past 21000 Years based on the TraCE-21ka simulations. *Journal of Climate*, *33*(17), 7455–7478. https://doi.org/10.1175/JCLI-D-19-0798.1

Matero, I. S. O., Gregoire, L. J., Ivanovic, R. F., Tindall, J. C., & Haywood, A. M. (2017). The 8.2 ka cooling event caused by Laurentide ice saddle collapse. *Earth and Planetary Science Letters*, *43*(1), 205–214. https://doi.org/10.1016/j.epsl.2017.06.011

Railsback, L. B., Liang, F., Brook, G. A., Voarintsoa, N. R. G., Sletten, H. R., Marais, E., et al. (2018). The timing, two-pulsed nature, and variable climatic expression of the 4.2 ka event: A review and new high-resolution stalagmite data from Namibia. *Quaternary Science Reviews*, *186*(7–8), 78–90. https://doi.org/10.1016/j.quascirev.2018.02.015

Ruan, J., & Hu, C. (2010). Seasonal variations and environmental controls on stalagmite calcite crystal growth in Heshang Cave, central China. Chin. *Chinese Science Bulletin*, *55*(34), 3929–3935. https://doi.org/10.1007/s11434-010-4193-1

Scherrer, S. C., Valk, C. D., Begert, M., Gubler, S., Kotlarski, S., & Croci-Maspoli, M. (2024). Estimating trends and the current climate mean in a changing climate. *Climate Services*, *33*, 100428. https://doi.org/10.1016/j.cliser.2023.100428

Thomas, E. R., Wolff, E. W., Mulvaney, R., Steffensen, J. P., Johnsen, S. J., Arrowsmith, C., et al. (2007). The 8.2 kyr event from Greenland ice cores. *Quaternary Science Reviews*, *26*(1–2), 70–81. https://doi.org/10.1016/j.quascirev.2006.07.017

Wang, J., Lu, H., Cheng, J., & Zhao, C. (2023). Global terrestrial monsoon area variations since Last Glacial Maximum based on TraCE21ka and PMIP4-CMIP6 simulations. *Global and Planetary Change*, *231*, 104308. https://doi.org/10.1016/j.gloplacha.2023.104308